Sensors and Actuators A 165 (2011) 288–293

Contents lists available at ScienceDirect

Sensors and Actuators A: Physical

journal homepage: www.elsevier.com/locate/sna

A passive through hole microvalve for capillary flow control in microfluidic systems

Xin Du[a,b], Ping Zhang[a], Yongshun Liu[a], Yihui Wu[a,*]

[a] State Key Lab of Applied Optics, Changchun Institute of Optics, Fine Mechanics and Physics, Chinese Academy of Sciences, Changchun 130022, China
[b] Graduate School of Chinese Academy of Sciences, Beijing 100039, China

ARTICLE INFO

Article history:
Received 1 April 2010
Received in revised form 27 July 2010
Accepted 4 August 2010
Available online 11 August 2010

Keywords:
Passive microvalve
Through hole
Expansion angle
Contact angle
Microfluidics

ABSTRACT

A passive through hole microvalve is proposed to stop the capillary-driven flow in microchannels with small static contact angle ($\theta_s < 45^\circ$). Its gating condition on regulating flow is derived based on contact line theory. Using numerical simulations in certain limits and some experiments, we investigated the valve performance of a few different valve designs. A kind of converging through hole microvalve is found which can stop the relative faster capillary flow and is easier to fabricate and integrate. It is shown that allowable flow velocity for DI water could reach 0.5 m/s, and the height of microvalve could be as short as to 20 μm.

© 2010 Elsevier B.V. All rights reserved.

1. Introduction

The centrifugal "lab-on-a-disk" platform has been proposed as a kind of important microfluidic system because its artificial gravity field intrinsically implements a pumping force [1–3]. The platform can be widely used in the field of clinical diagnostics and drug discovery. Flow control on rotating disks is mainly achieved by passive capillary burst microvalve (CBV) because there are no requirements of moving parts, external power devices and electrical control. The first kind of such valves relies on the variation of static contact angle realized by depositing hydrophobic patches on the surface of an otherwise hydrophilic microchannel to block a flow until a specific rotational frequency is reached [4,5]. The second kind of CBVs is especially attractive, as it needs only a sudden expansion of the microchannel cross-section where the liquid meniscus is trapped at the beginning of the expansion [6,7]. It is insensitive to physicochemical properties of the liquid sample and easy to fabricate.

In planar microfluidic systems, it is quite common that the channel cross-section is rectangular or trapezoidal or limited by a flat cover [6–9]. Thus, it is often that not all of walls of a CBV are expansion and the flat cover makes the CBV work only when the static contact angle θ_s is greater than 45° [10–12]. In the case of $\theta_s < 45^\circ$, the liquid flows along the edges formed by the intersection of expansion section walls and the flat cover, and the CBV works only in a period of time and burst finally. Because the gravity effects can be safely neglected in horizontal microdevices [9], the microflow is similar to the capillary flow along an interior corner of a container under low gravity if the Concus–Finn condition is fulfilled [13].

For the successful commercialization of a microfluidic system, the designs of microvalves and other function parts of the system (i.e., the sample injection) need a comprehensive consideration. Because the injection will be easier for liquid sample with the smaller contact angle on the channel walls, the study of the CBV that can work with small static contact angle ($\theta_s < 45^\circ$) is very important.

A possible solution is a through hole on a flat surface. It provides an expansion at 360°. In current bulk micromaching process, the through hole is usually diverging due to micro-loading effect [14]. In this work, the gating condition of through hole CBV with an expansion angle is presented based on the contact line theory. The ability of stopping a capillary-driven flow is investigated by the numerical simulations of the capillary filling in microchannels with a dynamic contact angle [15,16]. Recently, 3-D CFD simulations have been successful by the volume of fluid (VOF) or level set method [17,18]. However, as the accuracy of the result is strongly dependent on the capture of liquid/gas interface, the 3-D model is still time costing and difficult to get the solution accurately. Here, a 1-D simplified model with the constant corner pressure assumption is used to get rapid design of the CBV. Some experiments are presented to help to obtain a valid range of the model. Finally, a kind of converging through hole CBV that could decrease the accuracy requirement of fabrication is presented.

* Corresponding author. Tel.: +86 0431 86176915; fax: +86 0431 85690271.
E-mail address: ciomp_yihuiwu@hotmail.com (Y. Wu).

0924-4247/$ – see front matter © 2010 Elsevier B.V. All rights reserved.
doi:10.1016/j.sna.2010.08.006

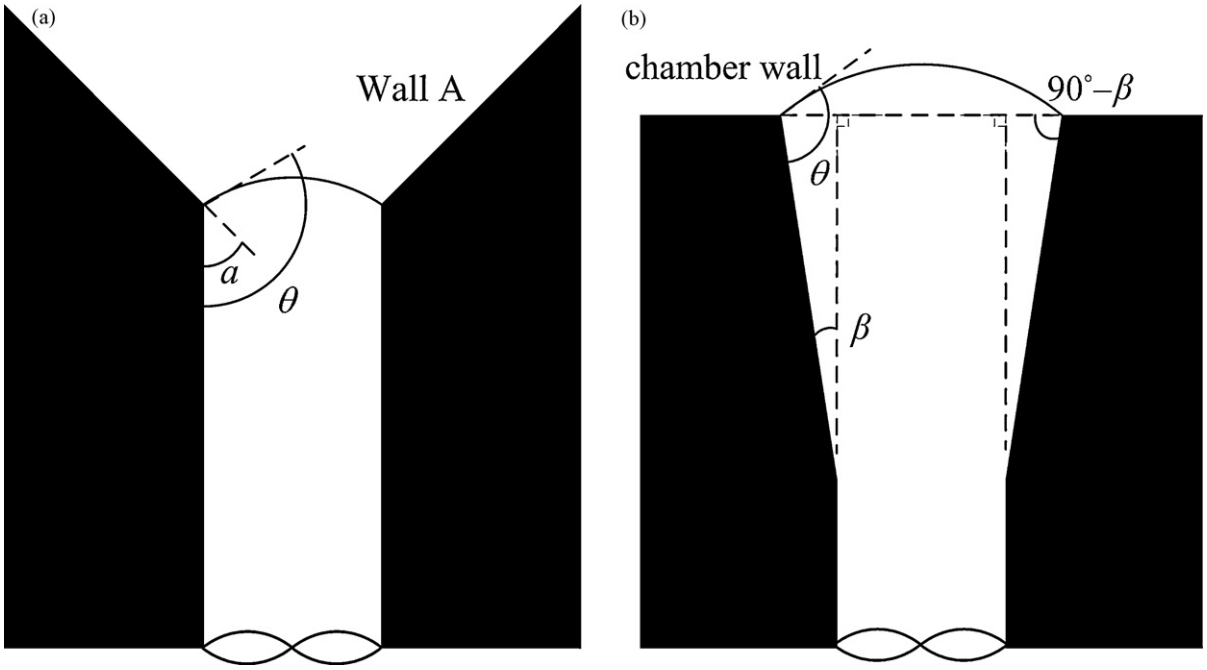

Fig. 1. Schematic representation of CBV. (a) Schematic representation of a CBV; (b) schematic representation of a diverging through hole CBV.

2. Analysis of the capillary burst valve

The static (equilibrium) contact angle shows the wettability of the solid surface. Because practically a hysteresis often arises, the static contact angle is not same when a meniscus over a substrate goes forward or backward. When the contact angle is between the advancing contact angle θ_A and receding contact angle θ_R, the wetting line stops [19].

For a hydrophilic circular tube with a sudden enlargement, as shown in Fig. 1a, the liquid will spontaneously advance in the straight tube with dynamic contact angle θ. When the liquid reaches the diverging section, the contact angle with the new wall (wall A in Fig. 1a) reduces to $\theta - \alpha$, where α is the tube expansion angle. If $\theta - \alpha$ is smaller than θ_A, the contact line will be stopped and be restarted until the contact angle with the new wall increases to the advancing contact angle θ_A. The valve then fails and the liquid burst through the valve.

Fig. 1b shows the scheme of a through hole CBV with an expansion angle β. When the liquid reaches the outlet of CBV, its contact angle with the chamber wall reduces from θ to $\theta + \beta - 90^\circ$, where θ is the dynamic contact angle with the wall of the through hole. When the contact angle with the chamber wall increases to the advancing angle θ_A, the CBV bursts and the meniscus proceeds on the chamber wall. Therefore, the gating condition for the diverging through hole CBV is

$$\theta + \beta - \theta_A - 90^\circ < 0 \quad (1)$$

The burst pressure is

$$\Delta p = \frac{2\sigma \cos(\theta_A + 90^\circ)}{r} \quad (2)$$

where σ is the surface tension, r is the radius of the outlet of the through hole.

3. Microchip design and experiments set-up

Several capillary-driven microfluidic systems were designed to study the CBV. The fluid penetrates from the inlet port into the entry flow microchannel without any additional external forces, and then goes forward to the through hole until it reaches the outlet of CBV where the valve's status is observed with a stereoscopic microscope. Fig. 2 shows the schematic diagram of the experimental device. The variation range of the through holes we obtained were from 90 μm to 235 μm for both their diameters and heights, their expansion angles were from −4° to 19°. The entry flow channels had a rectangular cross-section with fixed height (100 μm) and varied width (100–200 μm). The channel length was 3 mm, 4 mm, 5 mm, 10 mm, 15 mm, 25 mm, and 40 mm.

The liquid used in all experiments was de-ionized water. The advancing contact angle on the silicon surface cleaned by the mixtures of H_2SO_4/H_2O_2 (3:1) was 8°. The DI water was stained red with ink for convenient observation.

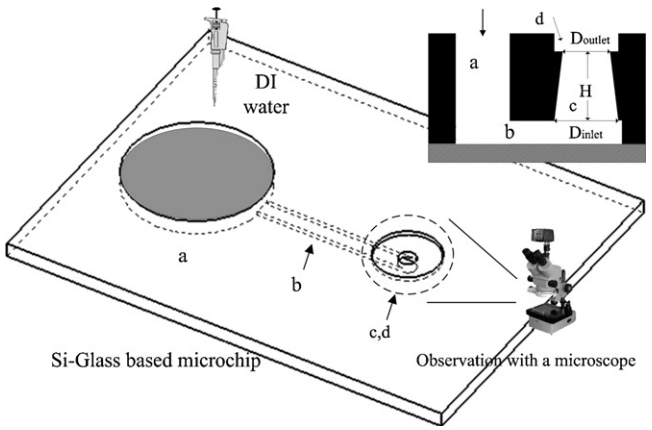

Fig. 2. Schematic diagram of the experimental device for observing the status of CBV. The microscope is focused on the outlet of CBV. The figure at the top-right is the section view of the device, a – inlet port; b – entry flow microchannel; c – through hole; d – reservoir chamber.

4. Method

4.1. Numerical simulation of the capillary filling

The Washburn equation applied in this section is for the computation of the average flow velocity. The capillary force pulls the fluid into the entry flow channel. Balancing the capillary forces against the viscous drag gives an expression for the position of the advancing fluid in the horizontal channel x as a function of time t [16],

$$\frac{32\mu}{D_H^2}x\dot{x} = \frac{4\sigma}{D_H}\cos\theta \tag{3}$$

where $\dot{x}$ is the flow speed, D_H is the hydraulic diameter and μ is liquid viscosity.

Considering the effect of the contact line velocity on the dynamic contact angle, the correlation by Jiang et al. [20], based on Hoffman's data [21], was

$$\cos\theta = \cos\theta_A + (1+\cos\theta_A)\tan h(4.96\mathrm{Ca}^{0.702}) \tag{4}$$

where $\mathrm{Ca} = (\mu\dot{x})/\sigma$ is the capillary number.

After passing the corner with a right angle, the liquid penetrates into the vertical through hole. The pressures at the both ends of the liquid flow in the through hole are the corner pressure p_c and the atmospheric pressure p_0, respectively. The control equation is

$$\frac{32\mu}{D^2(y)}y\dot{y} = p_c - \left(p_0 - \frac{4\sigma}{D(y)}\cos\theta\right) \tag{5}$$

where y is the length of the liquid sample in the vertical through hole, $D(y) = D_{inlet}\cdot(1+y\tan\beta)$ is the hole diameter at the meniscus, D_{inlet} is the diameter of the inlet of the through hole.

When the liquid just arrived at the corner, the variation of moment of the liquid flow in the horizontal entry flow channel could be considered in the following way. After a small time increment Δt, a fluid microelement at the corner stopped rapidly in the horizontal direction from the flow velocity $\dot{x}_L$ and the equal mass fluid microelement was supplemented into the entry flow channel from inlet port because of the liquid's incompressibility. As the flow speed of the rest of the liquid flow changed slightly, the variation was ignored. By the moment theorem in the horizontal direction,

$$(p_c - p_0)A + \frac{32\mu}{D_H}x\dot{x}_L - \frac{2\sigma}{D_H}\cos\theta = \rho\dot{x}_L A(0-(-\dot{x}_L)) \tag{6}$$

where ρ is the liquid density, A is the area of the channel cross-section, $\dot{x}_L$ is the entry flow speed at the end of entry flow channel.

As the viscosity force is counteracted by the capillary force based on Eq. (3), the corner pressure at the moment when the liquid just arrived at the corner can be obtained as

$$p_c = p_0 + \rho\dot{x}_L^2 \tag{7}$$

The variation of corner pressure is difficult to determine (due to the complex flow field) and therefore a simple zero order model of corner pressure is adopted.

$$p_c(t) = p_c(0) = p_0 + \rho\dot{x}_L^2 \tag{8}$$

The initial condition is

$$x \text{ or } y = 0, \quad \text{at } t = 0 \tag{9}$$

Using this condition would yield a singularity. Instead, the numerical integration is started at $x = 10^{-11}$ m. The simulation was carried out by mathematical software package (Matlab R14)

4.2. Fabrication method

The fabrication processes were composed of ICP etch, electroforming, evaporation and anodic bonding. As shown in Fig. 3, in a silicon wafer, the entry flow microchannels on the back of the microchip were generated firstly by standard process of photolithography and ICP etch (Alcatel 601E ICP reactor). Then a 1 μm Cu layer was covered the channels for protection by the electroforming process. Next, the through holes and the reservoir chambers linking the outlet of CBVs on the front of the microchip were obtained by a two-level technology of silicon etching as described by Ajmera etc [9,22]. The through hole obtained is usually diverging due to the micro-loading effect. Finally, the silicon wafer was bonded with a Pyrex glass wafer by the anodic bonding process (SUSS SB6 bonder).

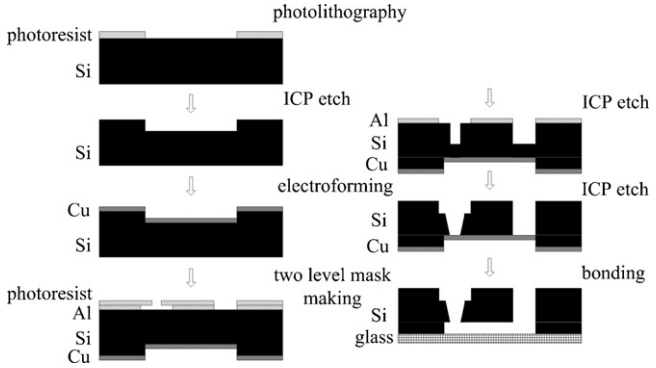

Fig. 3. Process diagram of through hole CBV (the through hole obtained is diverging).

But if we change the process order of the fabrication that the reservoir chambers on the front of the microchip was etched firstly, thus the entry flow channels on the back of microchip and the through holes were fabricated synchronously, and the converging through hole CBVs will be obtained. A scanning electron microscopy image in Fig. 4 shows an example of a converging through hole CBV fabricated by this process.

5. Results and discussion

5.1. 1-D model validation

To vary the length of the entry flow channel can provide different entry flow velocity $\dot{x}_L$ and capillary number Ca when the liquid just reaches the corner. Table 1 shows the experimental results of the status of CBVs with different expansion angles when the length of entry flow channel L or capillary numbers $\mathrm{Ca} = \dot{x}_L\mu/\sigma$ is taken as the control parameter. The obtained expansion angles for the same group in Table 1 have $\pm1^\circ$ fluctuation. The results confirmed the analysis based on the inequality (1). When a CBV is given, the allowable capillary number of entry flow is limited. The CBVs with relative smaller expansion angle have better valve abilities of stopping a flow. Except of the expansion angle, the influences of the height and inlet diameter of CBVs on the valve status also need to be included when the length of entry flow channels is smaller than 4 mm.

The values of the expression $\theta+\beta-\theta_A-90^\circ$ at the outlet of CBVs are shown in Fig. 5 as a function of the length of a entry flow channel based on the Eqs. (3)–(8). The valve will burst when $\theta+\beta-\theta_A-90^\circ>0$. The sizes of CBVs and microchannels from Table 1 are used. The expansion angle used in simulation was set as the average value β (black line), the fluctuation range $\beta+1^\circ$ (red line) and $\beta-1^\circ$ (blue line), respectively, for each group in Table 1.

The simulations show that the variation of expression $\theta+\beta-\theta_A-90^\circ$ is very small when the allowable channel length is rather long, for example longer than 4 mm. At this condition, the influence of entry flow channel on the status of CBV is small and the simulations of the allowable channel length are consistent with the experimental data. When the channel length is smaller

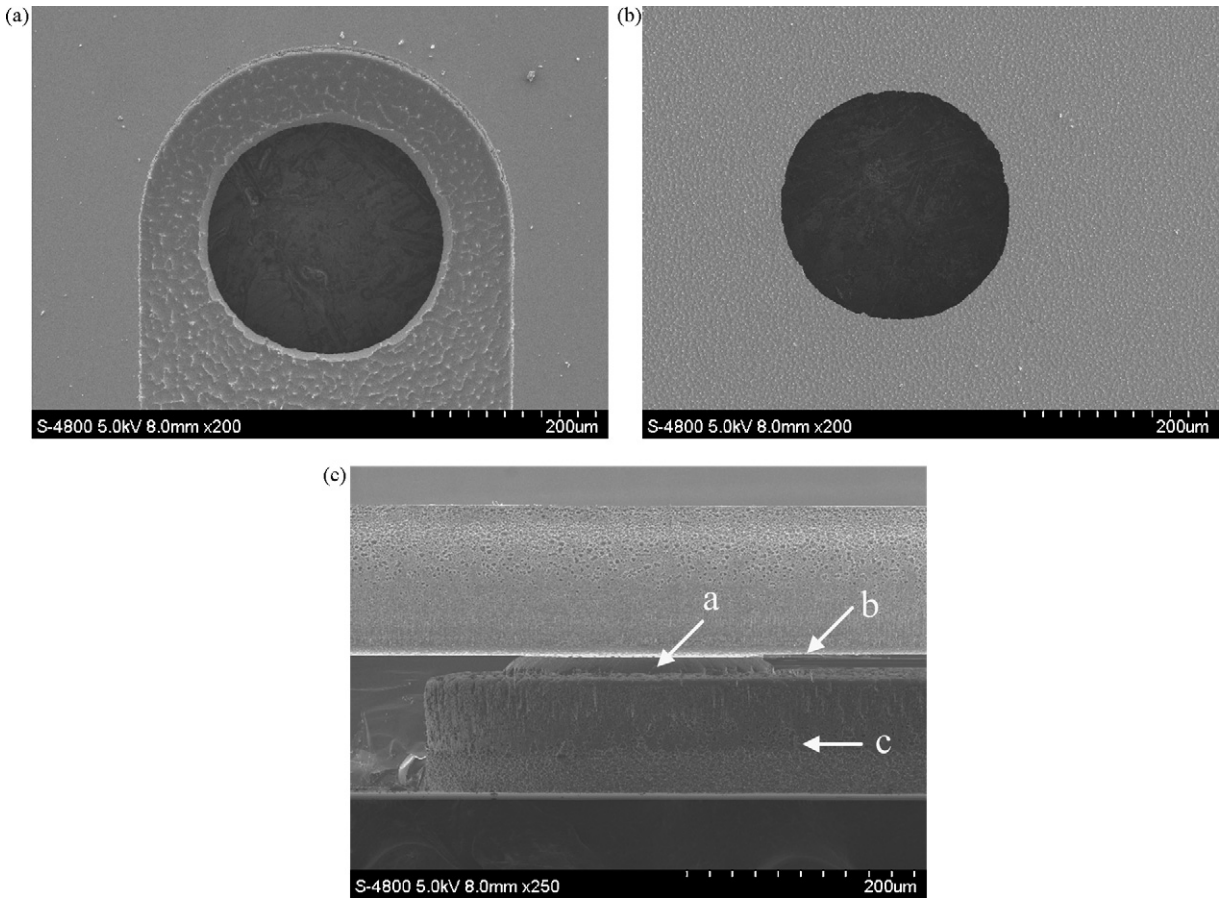

Fig. 4. Scanning electron microscopy pictures of a converging CBV sample: (a) the bottom view; (b) the top view; (c) the section view. The pictures are corresponding to the part of the circle in Fig. 2. a – through hole; b – chamber wall; c – entry flow channel.

than 4 mm, some results from simulation are different from our experiments. It may be attributed to the constant corner pressure assumption that the pressure variation at the inlet of CBV is ignored. The approach is reasonable when the valve's performance is affected more by the features of the through hole (expansion angle, height and inlet diameter) than the characters of the entry flow. When the entry flow speed increases and the height of the through hole decreases, the effect of entry flow becomes a dominant factor. For more accurate model, the effect of inertia item should be included.

5.2. The operating characteristics of CBV

For a better insight on the operating characteristics of CBV, calculations were carried out by changing the sizes of through holes and entry flow channels. Here, we consider the valves whose diameters are larger than 100 μm. For the applications of interest, the burst pressure of the valves is more than 100 Pa, thus the inlet diameters of CBVs are smaller than 400 μm based on Eq. (2). Considering the thickness of the silicon wafer, the heights of CBVs are chosen to be less than 200 μm.

Table 1
The status of CBVs with different entry flow channels.

Test group	CBV			Microchannel			Ca	CBV status
	Divergent angle β/°(±1°)	Inlet diameter D/μm	Hole depth/μm	Width/μm	Height/μm	Length/μm		
1	15(−1)	215	120	210	115	5	3.7×10^{-3}	Burst
	15(+0)	215	120	210	115	10	1.8×10^{-3}	Burst
	15(+1)	215	120	210	115	15	1.2×10^{-3}	Work
	15(+1)	215	120	210	115	25	0.9×10^{-3}	Work
2	18(+1)	90	110	105	115	10	1.4×10^{-3}	Burst
	18(−1)	90	110	105	115	15	0.9×10^{-3}	Work
	18(+0)	90	110	105	115	25	0.5×10^{-3}	Work
3	2(+0)	205	183	195	100	3	4.3×10^{-3}	Work
	2(+0)	205	183	195	100	4	3.3×10^{-3}	Work
4	−3(+0)	215	90	205	100	3	4.0×10^{-3}	Burst
	−3(+1)	215	90	205	100	4	3.4×10^{-3}	Work

Notes: Fluctuation range: $\Delta\beta \leq 1°$, Δw, $\Delta D \leq 5$ μm, $\Delta h \leq 1$ μm.

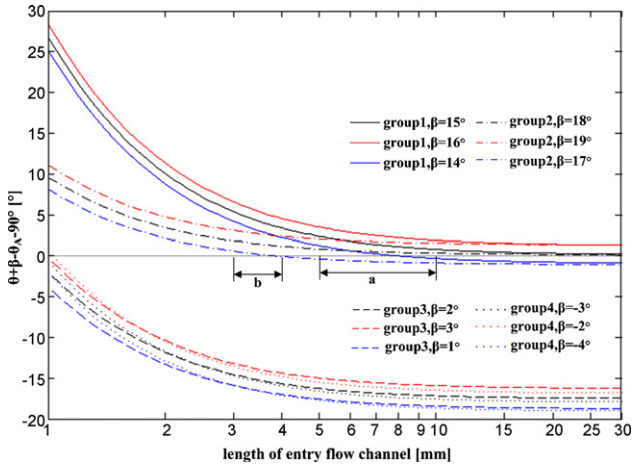

Fig. 5. Influence of the length of entry flow channel for different expansion angle (the test liquid was DI water, $\theta_A = 8^\circ$). a – experiment data for groups 1,2; b – experiment data for group 3.

For the entry flow channels, the sizes are chosen with the height from 50 μm to 200 μm, the width from 100 μm to 800 μm, and the length from 1 mm to 20 mm. Based on Eqs. (3)–(4), the probable flow velocity $\dot{x}_L$ at the end of channel is from 0.03 m/s to1.26 m/s, thus the corresponding dynamic pressure item $\rho\dot{x}_L^2$ is in 0–1.6 KPa.

When the expansion angle is given, the maximum of allowable dynamic contact angle at the outlet of CBV is determined by inequality (1). Based on Eqs. (4)–(8), the probable maximum dynamic pressure item can be obtained when the others sizes (the inlet diameter D_{inlet} and hole height h) of through hole are given, as shown in Fig. 6. The allowable entry flow speed is a continuous decreasing function of the expansion angle. When the flow speed decreases to zero, which means the allowable channel length is far out of the size limit of microfluidic devices, the cut-off expansion angle β_{max} is obtained. In this condition, the allowable expansion angle reaches its maximum when the ratio of D_{inlet}/h is smallest. The value of β_{max} is about 20° (for the case of $D_{inlet} = 100$ μm, $h = 200$ μm). As the simulation has a large deviation when the length of channel is smaller than 4 mm, the corresponding dynamic pressure item $\rho\dot{x}_L^2$ is smaller than 0.25 KPa. The qualitative description is shown in Fig. 6 that the valve with small ratio of D_{inlet}/h and small expansion angle is good for a better performance of stopping a flow.

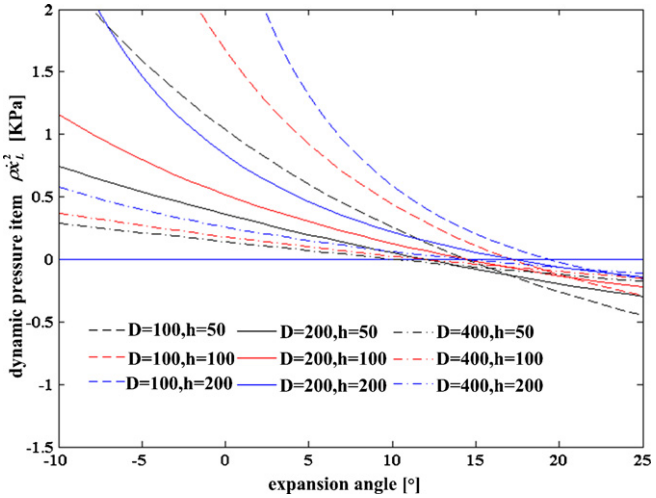

Fig. 6. Influence of the expansion angle (the unit of through holes is μm).

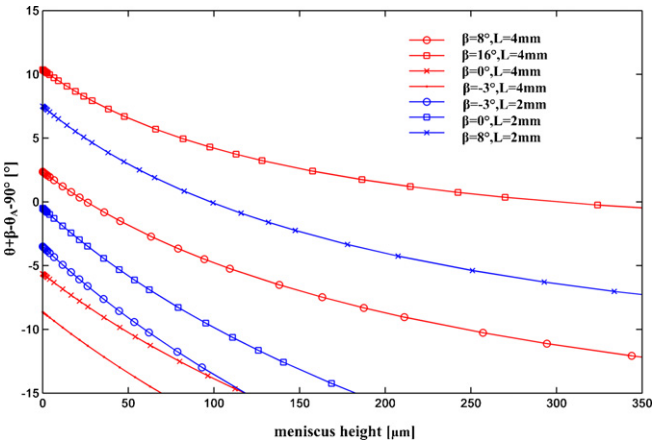

Fig. 7. Influence of the height of the meniscus in a through hole ($\theta_A = 8^\circ$; $L = 2, 4$ mm, $w = 200$ μm, $h = 100$ μm for the entry flow channel; $D_{inlet} = 200$ μm for the through hole).

5.3. The converging through hole CBV

The variation of expression $\theta + \beta - \theta_A - 90^\circ$ at the liquid meniscus with the increasing of the height of the meniscus in the vertical through hole is shown in Fig. 7. For a given entry flow channel, the allowable height of the through hole reduced rapidly when the expansion angle decreased. In the case of that the entry flow channel is 4 mm × 200 μm × 100 μm (length × width × height), the allowable height of through hole is smaller than 30 μm when the expansion angle is smaller than θ_A. When the length of channel decreased to 2 mm, the CBV with the same expansion angle and inlet diameter requires the larger height of through hole than the case of 4 mm. Let us notice that the height and expansion angle of through hole will not influence the status of CBV when the valves have a converging through hole, $\beta < 0$.

Based on the above analysis, a converging through hole CBV is presented. Table 2 gives the experimental results for the valve ability of converging CBVs. The valves with only 20 μm height worked effectively when the channel length is more than 4 mm (correspondingly, $\dot{x}_L = 0.5$ m/s). There is a great agreement with the simulation results obtained by constant corner pressure approach. However, when the channel length is smaller than 3 mm, most of the CBVs burst and the height from computation has a large deviation from the experimental results.

In fact, when the effect of entry flow channel is ignorable, the dynamic contact angle for a capillary flow in a through hole is usually smaller than 90° because the capillary is a driving force. When $\beta < \theta_A$, the gating condition of CBV is fulfilled and the valve does always work. When the channel length is short, the effect of dynamic pressure becomes significant and the dynamic contact angle of liquid in a through hole can be larger than 90°. Thus, the smaller expansion angle and the greater height of through hole are required. Because the constant corner pressure assumption is no

Table 2
The status of converging through hole CBV with different entry flow channels.

D_{inlet} (μm)	100		200			400		
W (μm)	100	200	100	200	400	200	400	800
L (mm)								
5	√	√	√	√	√	√	√	√
4	√	√	√	√	√	√	√	√
3	√	×	×	×	√	√	×	×
2	×	×	×	×	×	×	×	×

Notes: √ – CBV works; × – CBV burst. The height of the through hole is 20 μm, expansion angle $\beta = -60^\circ$ to 0°; the height of the entry flow channel is 90 μm.

longer valid when the length of entry flow channel is smaller than 4 mm, the predictions in these cases had poor agreements with the experiment data.

6. Conclusion

In this study, the gating condition of through hole CBV with an expansion angle is presented based on the contact line theory, which is $\theta + \beta - \theta_A - 90^\circ < 0$. The microfluidic devices are designed to operate with the capillary-driven DI water flow. A 1-D model with constant corner pressure assumption is used to study the valve performance of CBVs. When the characteristic size of the CBVs and microchannels are a few of hundred micrometers, the simulations agreed well with the experimental results with a long entry flow channel that is longer than 4 mm which means the influence of entry flow is a small factor for CBV at this condition. Based on the simulate results, the CBVs with smaller expansion angles have better ability of stopping a flow and the allowable maximum expansion angle should be less than 20° when the inlet diameter of the through hole is larger than 100 μm and the height is smaller than 200 μm. A kind of converging through hole CBV is presented. The valve can work efficiently when the entry flow velocity is smaller than 0.5 m/s and the height of through hole could be decreased to 20 μm. Because the value of the expansion angle is not limited, the converging CBV decreases greatly the difficulties of the fabrication process.

Acknowledgements

This work was supported by grants from the National High Technology Research and Development Program of China (Grant numbers 2006AA04Z367, 2007AA042102), the National Science Foundation of China (Grant number 60971025), and Knowledge Innovation Program of Chinese Academy of Sciences (Grant number KJCX2-YW-H18).

References

[1] M.J. Madou, G.J. Kellogg, Proceedings of SPIE, vol. 3259, LabCD: a centrifuge-based microfluidic platform for diagnostics, 1998, pp. 80–93.
[2] D.C. Duffy, H.L. Gillis, J. Lin, N.F. Sheppard, G.J. Kellogg, Microfabricated centrifugal microfluidic systems: characterisation and multiple enzymatic assays, Anal. Chem. 71 (20) (1999) 4669–4678.
[3] J. Ducrĭee, S. Haeberle, S. Lutz, S. Pausch, F. von Stetten, R. Zengerle, The centrifugal microfluidic Bio-Disk platform, J. Micromech. Microeng. 17 (2007) 103–115.
[4] H. Andersson, W. van der Wijngaart, P. Griss, F. Niklaus, G. Stemme, Hydrophobic valves of plasma deposited octafluorocyclobutane in DRIE channels, Sens. Actuators B: Chem. 75 (2001) 136–141.
[5] J. Steigert, S. Haeberle, T. Brenner, C. Müller, C.P. Steinert, P. Koltay, N. Gottschlich, H. Reinecke, J. Rühe, R. Zengerle, J. Ducrĭee, Rapid prototyping of microfluidic chips in COC, J. Micromech. Microeng. 17 (2007) 333–341.
[6] P.F. Man, C.H. Mastrangelo, M.A. Burns, D.T. Burke, Microfabricated capillary driven stop valves and sample injector, MEMS Conference, Heidelberg, Germany, January 25–29, 1998.
[7] H. Cho, H.Y. Kim, J.Y. Kang, T.S. Kim, How the capillary burst microvalve works, J. Colloid Interface Sci. 306 (2007) 379–385.
[8] T.S. Leu, P.Y. Chang, Pressure barrier of capillary stop valves in micro sample separators, Sens. Actuators A: Phys. 115 (2004) 508–515.
[9] A. Glière, C. Delattre, Modeling and fabrication of capillary stop valves for planar microfluidic systems, Sens. Actuators A: Phys. 130 (2006) 601–608.
[10] M. Zimmermann, P. Hunziker, E. Delamarche, Valves for autonomous capillary systems, Microfluid. Nanofluid. 5 (2008) 395–402.
[11] T. Metz, J. Viertel, C. Müller, S. Kerzenmacher, N. Paust, R. Zengerle, P. Koltay, Passive water management for μfuel-cells using capillary microstructures, J. Micromech. Microeng. 18 (2008), 104007 (10pp).
[12] R. Seemann, M. Brinkmann, E.J. Kramer, F.F. Lange, R. Lipowsky, Wetting morphologies at microstructured surface, Proc. Natl. Acad. Sci. 102 (2005) 1848–1852.
[13] P. Concus, R. Finn, On capillary free surfaces in the absence of gravity, Acta. Math. 132 (1974) 177–198.
[14] C. Hedlund, H.O. Blom, S. Berg, Microloading effect in reactive ion etching, J. Vac. Sci. Technol. A 12 (1994) 1962–1965.
[15] W.-B. Young, Analysis of capillary flows in non-uniform cross-sectional capillaries, Colloids Surf. A: Physicochem. Eng. Aspects 234 (2004) 123–128.
[16] R. Chebbi, Dynamics of liquid penetration into capillary tubes, J. Colloid Interface Sci. 315 (2007) 255–260.
[17] G. Silva, N. Leal, V. Semiao, Critical pressure for capillary valves in a Lab-on a-Disk: CFD and flow visualization, Comp. Struc., doi:10.1016/j.compstruc.2009.01.014.
[18] A.A. Saha, S.K. Mitra, Effect of dynamic contact angle in a volume of fluid(VOF) model for a microfluidic capillary flow, J. Colloid Interface Sci. 339 (2009) 461–480.
[19] D. Bonn, J. Eggers, J. Inderkeu, J. Meunier, E. Rolley, Wetting and spreading, Rev. Modern Phys. 81 (2009) 739–805.
[20] T.S. Jiang, S.-G. Oh, J.C. Slattery, Correlation for dynamic contact angle, J. Colloid Interface Sci. 69 (1979) 74–77.
[21] R.F. Hoffman, A study of the advancing interface. I. Interface shape in liquid–gas systems, J. Colloid Interface Sci. 50 (1975) 228–241.
[22] S.K. Ajmera, C. Delattre, M.A. Schmidt, K.F. Jensen, Microfabricated cross-flow chemical reactor for catalyst testing, Sens. Actuators B: Chem. 82 (2002) 297–306.

Biographies

Xin Du obtained his BSs degree in mechanics from the University of Science and Technology of China, Hefei, China, in 1998 and his MSc degree in fluid mechanics from Institute of Mechanics, Chinese Academy of Sciences, Beijing, China, in 2001. He is currently a PhD candidate at Changchun Institute of Optics, Fine Mechanics and Physics, Chinese Academy of Sciences, Changchun, China. His work is focused on fabrication and characterization of microfluidic devices with biochemical diagnostics.

Ping Zhang obtained her BSs degree in semiconductor physics from the Jilin University in 1982. From 1982 to 1999, she worked in Changchun institute of physics, Chinese Academy of Sciences. She is presently working on microfluidic chip and biochemical sensor by ICP technique and soft lithography in State Key Lab of Applied Optics, Changchun Institute of Optics, refined Mechanics and Physics, Chinese Academy of Sciences.

Yongshun Liu obtained his BSs degree in Microelectronics from the Jilin University in 2005. Since 2005, he has been a research associate involved in microfluidic chip and biochemical sensor research by Si microfabrication technique and soft lithography in State Key Lab of Applied Optics, Changchun Institute of Optics, refined Mechanics and Physics, Chinese Academy of Sciences.

Yihui Wu obtained her BSs degree in engineering from Tianjin Science and Technology University in 1986 and her master and PhD degrees in engineering from Changchun Institute of Optics, Fine Mechanics and Physics, Chinese Academy of Sciences in 1991 and 1996 respectively. She is a professor of the State Key Lab of Applied Optics, Changchun Institute of Optics in China. Currently her main research interests are microfluidic system, optical and acoustic biosensors and micro spectrometers, ect..